ACS OMEGA

Article

Cite This: ACS Omega 2019, 4, 2804−2811

http://pubs.acs.org/journal/acsodf

Chemical Postdeposition Treatments To Improve the Adhesion of Carbon Nanotube Films on Plastic Substrates

Ana Santidrián,[†] Olga Sanahuja,[†] Belén Villacampa,[‡] Jose Luis Diez,[§] Ana M. Benito,[†] Wolfgang K. Maser,[†] Edgar Muñoz,[†] and Alejandro Ansón-Casaos*[,†]

[†]Instituto de Carboquímica ICB-CSIC, Miguel Luesma Castán 4, 50018 Zaragoza, Spain

[‡]Departamento de Física de la Materia Condensada, ICMA, Universidad de Zaragoza-CSIC, Pza. S. Francisco s/n, 50009 Zaragoza, Spain

[§]Laboratorio de Microscopías Avanzadas (LMA), Instituto de Nanociencia de Aragón, Universidad de Zaragoza, C/Mariano Esquillor Gómez, s/n, 50018 Zaragoza, Spain

ABSTRACT: The robust adhesion of single-walled carbon nanotubes (SWCNTs) to plastic substrates is a key issue toward their use in flexible electronic devices. In this work, semitransparent SWCNT films were prepared by spray-coating on two different plastic substrates, specifically poly(ethylene terephthalate) and poly(vinylidene fluoride). The deposited SWCNT films were treated by dipping in suitable solvents separately, namely, 53% nitric acid (HNO_3) and *N*-methyl pyrrolidone. Direct evidence of SWCNT adhesion to the substrate was obtained by a peel-off test carried out with an adhesive tape. Moreover, these treatments caused enhanced film transparency and electrical conductivity. Electron microscopy images suggested that SWCNTs were embedded in the plastic substrates, forming a thin layer of conductive composite materials. Raman spectroscopy detected a certain level of doping in the SWCNTs after the chemical treatments, which particularly affected metallic nanotubes in the case of the HNO_3 treatment. The microscopic adhesion and hardness of the SWCNT films were studied through a nanoscratch test. Overall, the efficiency of selected chemical postdeposition treatments for improving the SWCNT adhesion and the robustness of the resulting SWCNT films are demonstrated on flexible substrates of different chemical compositions.

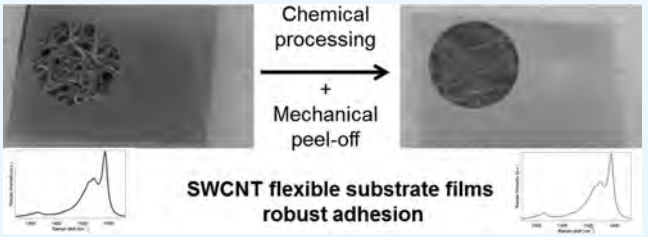

INTRODUCTION

Due to their remarkable structural and physical properties at the nanoscale (high electrical conductivity, tensile strength, flexibility, elasticity, thermal conductivity, high chemical stability, and low thermal expansion coefficient), carbon nanotubes (CNTs) and graphene are promising candidates for the development of novel electronic devices,[1,2] in particular, for the fabrication of functional transparent conducting films (TCFs).[3] Potential applications of CNT-TCFs include thin-film transistors, electronic displays, solar cell components, electroluminescent devices, supercapacitors, and sensors.[4] In addition, CNT-TCFs have been proposed as an alternative to indium tin oxide, being more easily incorporated on flexible substrates.[5−7]

Several methods are currently being utilized to fabricate CNT-TCFs, including direct CNT growth by chemical vapor deposition (CVD) and CNT deposition from liquid dispersions. Remarkable progress has been recently achieved using CVD methods, particularly by the dry floating catalyst technique.[8] On the other hand, dispersion techniques are versatile and suitable for many different manufacturing processes.[9] In particular, spray-coating is one of the most popular since it is simple, cost effective, repeatable, and can be easily scaled up.[10]

A good CNT adhesion to the substrate is an essential requirement toward CNT applications in electronics. A lack of chemical and mechanical stability in the functional films limits their applications, whereas film robustness extends the device lifetime. Several physical treatments have been tested to boost the CNT-TCF adhesion, such as the use of acrylic binders,[11] deposition of an interlayer,[12] hot pressing transfer process,[13] and microwave irradiation,[14] to name a few. Azoubel and Magdassi improved the adhesion of single-walled carbon nanotubes (SWCNTs) deposited on poly(ethylene terephthalate) (PET) by dipping in various acids, including nitric acid.[15] Similar treatments with oxidant acids have also shown to enhance the electrical conductivity of CNT-TCFs.[16−18] The increase in electrical conductivity has been attributed both to a p-type doping and to a decrease in the cross-junction resistance between CNTs.[19,20]

In this work, we further explore the use of TCF immersion methodologies to improve the SWCNT film adhesion on flexible polymer substrates, specifically poly(vinylidene fluoride) (PVDF) and PET. We here show that an optimized postdeposition treatment with nitric acid is valid for SWCNT-

Received: December 12, 2018
Accepted: January 15, 2019
Published: February 6, 2019

DOI: 10.1021/acsomega.8b03475
ACS Omega 2019, 4, 2804−2811

TCFs on plastics that are sensitive to oxidation, such as PET. PVDF provides remarkable electromechanical and dielectric properties and high chemical stability for biological and outdoor electronic applications.[21−23] However, nitric acid treatments are not useful for the relatively inert substrate PVDF, which is resistant to most inorganic solvents, aliphatic and aromatic hydrocarbons, organic acids, alcohols, and halogenated solvents. Only some dipolar aprotic solvents, such as dimethylformamide (DMF) or *N*-methyl-2-pyrrolidone (NMP), dissolve PVDF.[24]

It is here demonstrated that postdeposition immersion methods can be generalized to provide a robust adhesion of SWCNTs on different plastic substrates. A peel-off test performed with an adhesive tape is used as a first evidence of adhesion improvement. Besides, it is shown that the peel-off process can be considered a strategy for the removal of the excess SWCNT from the film after the immersion treatment. The effects of the immersion treatment and the peel-off process are discussed in terms of film transparency, electrical conductivity, thickness, morphology, and hardness, as well as the possible SWCNT doping.

RESULTS AND DISCUSSION

Transparency and Sheet Resistance. Films of SWCNTs on PET and PVDF substrates were prepared by spray-coating, as it is described in the Experimental section. By adjusting spray-gun parameters, such as air pressure, liquid flow, and distance to the substrate, uniform films were fabricated, which were ready for the immersion treatments and adhesion assessment.

Prior to the attainment of the results presented in this article, the immersion time and the solution composition were optimized. The immersion time was varied from 5 to 180 min. Concentrations of nitric acid in the range of 35−65% were tested for SWCNT-PET films. Besides, it was confirmed that no effect was produced on SWCNT adhesion to PVDF by dipping in nitric acid. Thus, solvent mixtures of DMF and NMP in the whole concentration range were tested for SWCNT-PVDF films. According to direct inspection and the adhesive tape test, the optimal conditions were found to be 52% HNO_3 and 120 min for SWCNT-PET films and 100% NMP and 50 min for SWCNT-PVDF films. The results of the peel-off experiments are shown in Figure 1. It has to be commented that too high HNO_3 concentrations or long treatment times may lead to damage in the plastic substrate.

The transparency at 550 nm (T) and sheet resistance (R_s) values of the SWCNT-TCFs were measured before and after the dipping treatment and the peel-off test (Figure 2). Typically, transparencies of the starting SWCNT films were

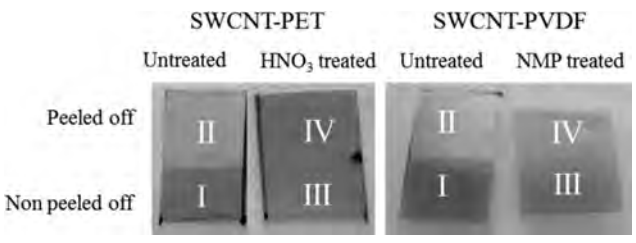

Figure 1. Effects of HNO_3 and NMP treatments on SWCNT-PET and SWCNT-PVDF films, respectively. Pictures of the films: I, as prepared; II, untreated and peeled off; III, immersion treated and nonpeeled off; IV, immersion treated and peeled off.

in the range of 50−60%, improving to nearly 70% after the immersion treatment and the peel-off process. Some variations can be observed in the value and trend of T and R_s parameters for SWCNT films on PET and PVDF, which might reflect the different properties of the substrates. Looking through SWCNT films, images are sharp but somewhat darkened. Thus, the films can be described as semitransparent. Quantification of the adhesion can be defined by an adhesion factor incorporating absorbance (A) data[25]

$$f = 1 - \frac{A_0 - A_n}{A_0} \quad (1)$$

where f is the adhesion factor, and A_0 and A_n are, respectively, the absorbance of the SWCNT film before and after the considered process. When $A_n = A_0$, $f = 1$ and no SWCNTs were lost in the process, therefore demonstrating perfect adhesion. On the contrary, when $f = 0$, no SWCNTs are left on the film, demonstrating no adhesion. The values of f for the specimen series are listed in Table 1.

According to Figure 2a, no substantial changes in the film transparency were observed comparing before ($f_I = 1$) and after the immersion treatments ($f_{III} = 1.06$). On the contrary, the transparency increased drastically when the untreated films were peeled off ($f_{II,PET} = 0.20$ and $f_{II,PVDF} = 0.07$ compared to f_I). As the SWCNT coating is removed from the substrate by the tape, the transparency increases, revealing poor adhesion. On the other hand, if the SWCNT film has good adhesion to the plastic substrate, the SWCNT coating remains. In fact, once the films underwent the immersion treatments, the SWCNTs stuck to the substrates with fairly good adhesion ($f_{IV,PET} = 0.65$ and $f_{IV,PVDF} = 0.75$).

As it is observed in Figure 2b, together with the adhesion improvement, the electrical conductivity increased (the sheet resistance R_s decreased) after the immersion treatments. This reduction in R_s has been associated with the removal of the sodium dodecyl sulfate (SDS) surfactant and with electrical doping.[16−20] The possibility of doping effects will be later considered in the discussion of Raman spectroscopy results. Besides, R_s measurements also evidence the adhesion improvement with the treatment. When the peel-off test was performed on the untreated films, the SWCNTs were removed from the plastic substrates and, as a consequence, R_s values significantly increased. However, when the films were chemically treated, the SWCNT network connectivity largely remains after the tape test.

Thickness. Changes in the film absorbance can be associated with the thickness (t). Profilometry measurements were performed on a series of untreated SWCNT films, with different transparencies (in particular seven samples between 21.7 and 77.4% transmittance). Therefore, a calibration line (t vs A) was obtained to calculate film thicknesses from transmittance measurements (Table 1). An interesting conclusion that can be drawn from Table 1 is that dipping treatments on both PET and PVDF substrates lead to nearly identical results in terms of SWCNT-TCF thickness.

Direct measurements of the thickness in SWCNT-TCFs are quite challenging, and data for comparison are scarce in the literature. Most of the available reports in the field only present transparency as an indirect measurement, and the available thickness data are usually calculated through different assumptions. Itkis et al. calculated the thickness of SWCNT-TCFs prepared by vacuum filtration assuming a theoretical film

DOI: 10.1021/acsomega.8b03475
ACS Omega 2019, 4, 2804−2811

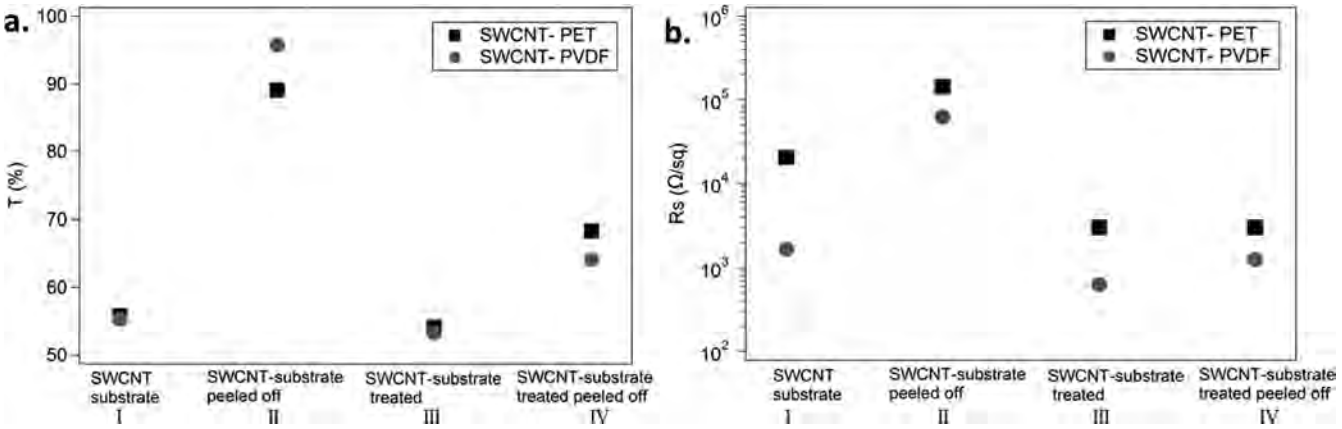

Figure 2. Effects of HNO_3 and NMP treatments on the transmittance at λ = 550 nm (a) and sheet resistance (b) of SWCNT-PET and SWCNT-PVDF films: I, as prepared; II, untreated and peeled off; III, immersion treated and nonpeeled off; IV, immersion treated and peeled off.

Table 1. Adhesion Factors (f), Thicknesses (t), and Bulk Conductivities (σ) of the SWCNT Films

film sample	f	t (nm)	σ (S cm^{-1})
SWCNT-PET as prepared—I	1	68	7
SWCNT-PET untreated peeled off—II	0.20	13	5
SWCNT-PET HNO_3 treated—III	1.06	72	46
SWCNT-PET HNO_3 treated peeled off—IV	0.65	45	75
SWCNT-PVDF as prepared—I	1	69	87
SWCNT-PVDF untreated peeled off—II	0.07	5	31
SWCNT-PVDF NMP treated—III	1.06	73	217
SWCNT-PVDF NMP treated peeled off—IV	0.75	52	154

bulk density.[26] These authors measured t values in the 0.5−8.0 nm range, which are quite lower than our data (Table 1). Closer values to our data were reported by Abdelhalim et al. by atomic force microscopy (AFM) on SWCNT-TCFs prepared by transfer printing on glass and plastic substrates (in the 10−25 nm range for 50−90% transparency).[6] Also, Li et al. measured t values of 40 nm by AFM for an SWCNT-TCF with a transparency of 78% at 550 nm.[27] Therefore, our perfilometer measurements are in good agreement with data reported by Abdelhalim et al. and Geng et al., although being somewhat larger at similar transparencies, which might be due to the different in-plane measurement ranges.

The bulk conductivity (σ) can be then calculated by measuring the film thickness (t) and sheet resistance (R_s) as

$$\sigma = 1/t{\cdot}R_s \quad (2)$$

The σ values are included in Table 1. In this work, σ values ranging from 46 to 220 S cm^{-1} have been calculated for the treated SWCNT-TCFs. The values are in good agreement with those deduced from Itkis et al.,[26] being approximately 40 and 450 S cm^{-1} for 33 and 99% metallic SWCNT-TCFs, respectively. Also, σ values of 48 and 83 S cm^{-1} are given by Tsai et al.[28] for CNT films with thicknesses of 230 and 110 nm, respectively. Somewhat higher σ values can be calculated from Li et al.,[27] reaching 550 and 2100 S cm^{-1} in water-washed and nitric acid treated SWCNT-TCFs, and from Abdelhalim et al.,[6] reaching 600−1600 S cm^{-1} for SWCNTs on a PET substrate and 1000−2600 S cm^{-1} on glass.

So far, the results evidence the beneficial effects of the immersion treatments in the SWCNT adhesion to the substrate and in the film's electrical conductivity as well. Besides, the peel-off process removes the excess of SWCNTs from the immersion-treated films, improving the transparency while maintaining the electrical conductivity. Therefore, the peel-off process can be considered as a method for the preparation of thin SWCNT-TCFs from the starting coatings.

Scanning Electron Microscopy (SEM) Characterization. From now on, further studies on the effect of dipping and peel-off treatments are presented only for the IV samples (Figure 1) in both PET and PVDF substrates and compared to the initial coatings (I samples in Figure 1). Actually, the peeled-off samples are the most appropriate ones for the present study, as adhesion phenomena take place in the deepest region of the original coating, where the SWCNTs are in close contact with the polymer surface during the immersion treatment.

SEM characterization studies (Figure 3) were conducted to identify changes in the SWCNT-TCF surface morphology. In all the cases, SWCNTs appear in the form of quite large bundles. An intense bundling effect of the SDS surfactant on SWCNT-TCFs has been previously revealed in comparison with other surfactants.[29] In spite of using the same initial SWCNT dispersion, PET and PVDF substrates lead to substantially different films since their respective surface properties are different.

In Figure 3a,c, a high density of SWCNT bundles is observed in the starting SWCNT-PET and SWCNT-PVDF films. However, a change in the film appearance occurs during the treatments (Figure 3b,d). The SWCNTs that were too far from the substrate (the deposited SWCNT excess) were removed during the peel-off test, so only the well-adhered SWCNTs remained. These stuck SWCNTs might be embedded within the PET and PVDF substrates, as it was suggested in previous works on PET,[15] and in a silica-type material after laser annealing.[30] Following those references, we suggest that HNO_3 and NMP might soften the surfaces of PET and PVDF, respectively, leading to the formation of a robust TCF of an SWCNT/polymer composite. Since the immersion time was optimized, SWCNTs would be embedded avoiding the substantial substrate damage. It is here demonstrated that the mechanism of SWCNT adhesion is nearly identical on PET and PVDF substrates, although the immersion treatment was performed in different solvents.

Raman Spectroscopy. Raman spectroscopy was performed for the identification of possible changes in the physical and chemical properties of SWCNTs that result from

DOI: 10.1021/acsomega.8b03475
ACS Omega 2019, 4, 2804−2811

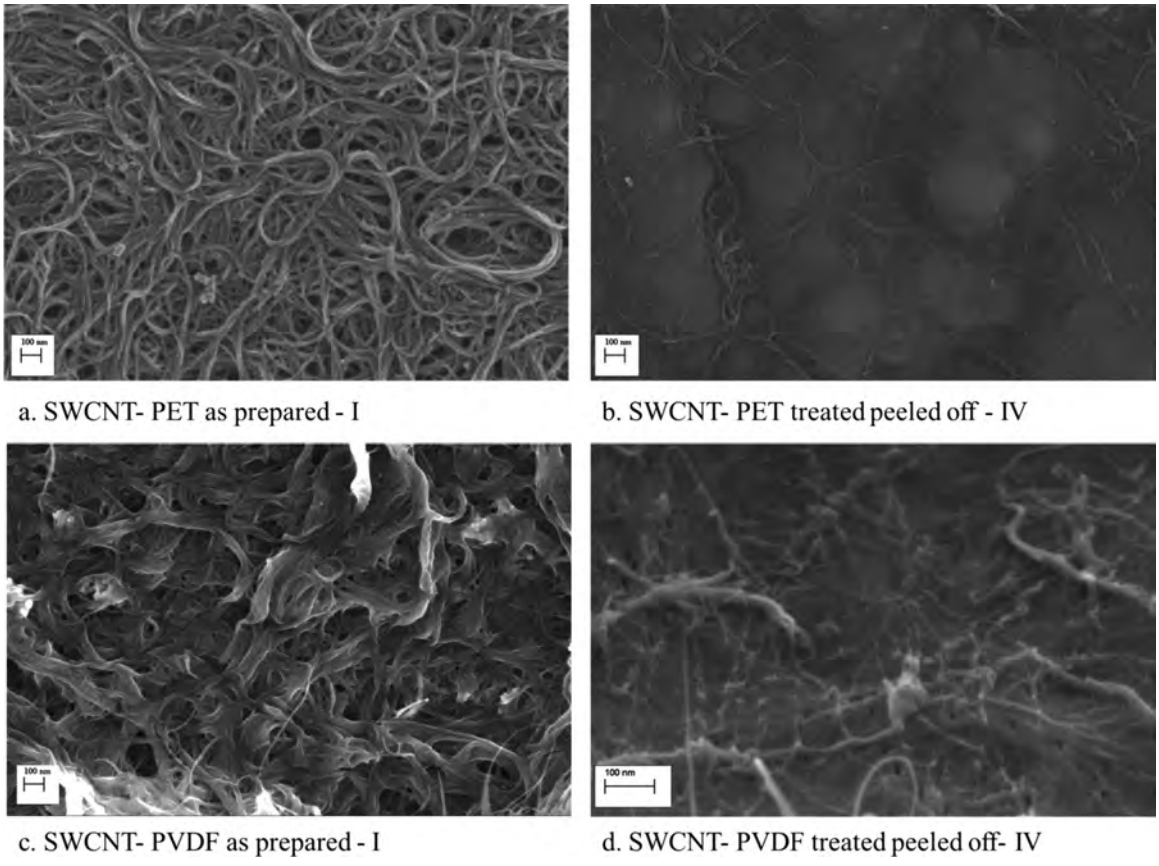

Figure 3. SEM images (scale bar = 100 nm) of SWCNT films on PET (a, b) and PVDF (c, d) before (a, c) and after (b, d) the immersion and peeling-off treatments.

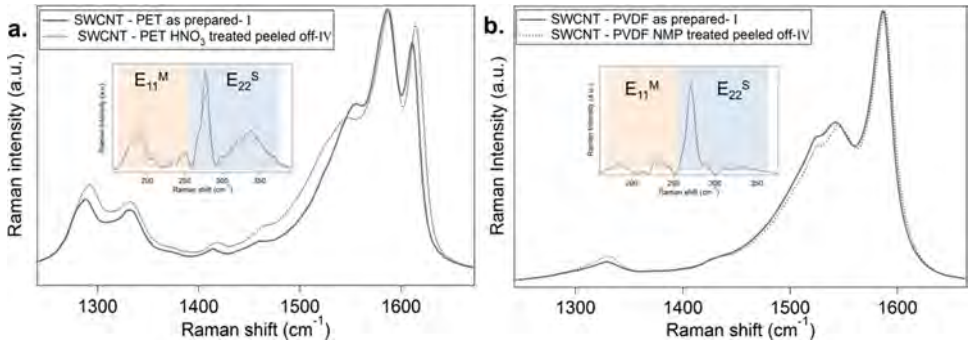

Figure 4. Resonance Raman spectra of SWCNT-PET (a) and SWCNT-PVDF (b) films before (line) and after (dots line) the immersion and peeling-off treatments.

the abovementioned chemical procedures, particularly in the optoelectronic properties and the occurrence of electronic doping. Spectra were acquired by mapping over 400 locations for each sample, using 2.33 eV laser excitation energy. The average profiles are represented in Figure 4. The Raman spectrum of SWCNTs presents several features, among which the most intense ones are the radial breathing modes (RBMs, Figure 4 insets), whose Raman shift ranges from 100 to 400 cm^{-1}, and the tangential modes (G-band) centered at 1588 cm^{-1}. Additionally, for SWCNTs containing structural defects, the disorder-induced mode (D-band) is observed at around 1330 cm^{-1}. In Figure 4a, the Raman spectra include contributions from the PET substrate at 1288, 1415, 1460, and 1615 cm^{-1}.

Using the RBM frequency, the diameter of SWCNTs (d_t) can be estimated.[31] The positions of the most intense RBM bands are in the following ranges: 165−210 cm^{-1} (d_t = 1.48−1.13 nm), 225−255 cm^{-1} (d_t = 1.05−0.93 nm), 255−295 cm^{-1} (d_t = 0.93−0.86 nm), and 300−340 cm^{-1} (d_t = 0.79−0.70 nm). Comparing the SWCNT-PET and SWCNT-PVDF films, the relative intensities of the RBM are different, which might be associated with the particular morphologies of the SWCNT deposits, as described above (Figure 3). The electronic transitions can be assigned using the Kataura plot.[32] The insets of Figure 4a,b are divided into two regions that correspond to SWCNTs excited via the E_{11}^{M} and E_{22}^{S} electronic transitions. Hence, certain semiconducting and metallic SWCNTs were in resonance with the 2.33 eV excitation energy. A change in the RBM intensity is observed

DOI: 10.1021/acsomega.8b03475
ACS Omega 2019, 4, 2804−2811

in the SWCNTs in resonance via the E_{11}^{M} for the SWCNT-PET HNO_3-treated film.

An increase in the D-band intensity is observed after the immersion treatments. It means that some defects were generated as a result of the treatment with HNO_3 and NMP, more remarkably in the case of HNO_3. However, the new defects introduced in the treated and peeled-off SWCNTs not only do not cause a decrease in the overall conductivity of the SWCNT-PET and SWCNT-PVDF films but, instead, also lead to increased conductivity values due to charge transfer doping and surfactant degradation induced by SWCNT dipping in nitric acid and NMP.[19,20]

The G-band was slightly but consistently blue-shifted from 1586 to 1589 cm^{-1} and from 1586 to 1588 cm^{-1} after the HNO_3 and NMP dipping treatments on SWCNT-PET and SWCNT-PVDF films, respectively. These upshifts can be understood as a consequence of doping and due to changes in the surface chemistry of specific SWCNTs. Thus, according to observations in the RBM, the changes induced by nitric acid treatments are particularly noticeable for metallic-type SWCNTs (165−210 cm^{-1}, d_t = 1.48−1.13 nm). Besides, the HNO_3-treated SWCNT-PET films presented changes in the G-band width compared to the untreated films, confirming small modifications in the metallic character of SWCNTs that can be related to the reactivity of metallic SWCNTs in nitric acid, in good agreement with previous literature.[33,34] As it was pointed above, doping by HNO_3 has been proposed to contribute to the reduction of the R_s values.[19,20] In addition, it is known that nitrogen containing solvents induce doping effects on SWCNTs.[35]

Therefore, both HNO_3 and NMP immersion treatments induce doping in SWCNTs and create some electronic distortion (defects). In particular, HNO_3 gives rise to a larger number of defects, probably due to its oxidant character. Under ambient conditions, metallic SWCNTs are more sensitive than semiconducting SWCNTs to the oxidative effect of HNO_3.

AFM Roughness and Scratch Test. The surface topographies of the SWCNT-PET and SWCNT-PVDF films (samples I and IV) were examined by AFM, and roughness parameters were obtained with AFM analysis software (Table 2). The average roughness (R_a) for the image is defined as the arithmetic average of the absolute values of the surface height deviations from the central plane. The R_a value is a measurement of surface homogeneity.

Table 2. R_a of the SWCNT Films Measured by AFM

film sample	R_a (nm)
SWCNT-PET as prepared—I	61
SWCNT-PET HNO_3 treated peeled off—IV	86
SWCNT-PVDF as prepared—I	421
SWCNT-PVDF NMP treated peeled off—IV	547

The R_a parameter for the SWCNT-PET film was significantly lower than for the SWCNT-PVDF film. The difference might be associated with the resulting morphology of the SWCNT deposit, which substantially varies for both substrates, according to SEM images (Figure 3). On the other hand, relatively small increases in the R_a values were detected after the peel-off process on both substrates. The R_a factor exceeds by far the nanotube bundle diameter, so the change has to be associated with the surface distribution of randomly oriented SWCNT aggregates and SWCNT/polymer aggregates. Therefore, the R_a values confirm the efficiency of the peel-off process in the uniform removal of the SWCNT excess layer. Also, the surface homogeneity has to be taken into account for the interpretation of the other AFM data.

A relatively hard AFM tip was utilized to evaluate the resistance of SWCNT-TCFs to indentation and scratch. When the cantilever tip moves along the surface ($X-Y$ axis), some material may be detached depending on the applied vertical force (Z-axis). The released material accumulates at the sides of the scratch line and in some regions of the scanned area. The AFM in a topography mode was used to examine the surface of the SWCNT-PET and SWCNT-PVDF films before and after the scratch experiments (Figure 5). Each sample was tested at nine forces from 0.5 to 25 μN, and a 10 × 10 μm^2 area was scanned at each loading force. Therefore, images in Figure 5 show the effects of scanning nine square regions in a 3 × 3 matrix, ordered by decreasing load from left to right and from top to down. It can be observed that the highest loads cause the largest damage to the substrate.

To analyze the effect of the scratch tests, an average depth was calculated for each 10 × 10 μm^2 area and plotted as a function of the normal load (Figure 6). The SWCNT-PET and SWCNT-PVDF films bear forces of 3 and 2 μN, respectively. An increasing damage occurs for higher loadings, independent of the immersion treatment. Since the scratch depth soon becomes larger than the SWCNT thickness, it is deduced that damage is being caused to the substrate. Only the initial damage at 3 and 2 μN, respectively, for PET and PVDF films might be associated with the SWCNT layer. Anyways, the chemical postdeposition treatments do not modify the force required to break the surface with the AFM tip.

The substrate damage, given by the scratch depths, logically increases with load. In both SWCNT-PET and SWCNT-PVDF films, the depth at analogous loads is lower for chemically treated samples. Therefore, the immersion treatment leads to an increase in the surface hardness, which might be associated with the improvement in the SWCNT-TCF adhesion to the substrate. Both the SWCNT-PET and SWCNT-PVDF films behave in analogous ways, indicating that the different chemical treatments produced analogous effects and thus analogous mechanisms against external mechanical forces. This fact confirms the suitability of generalizing the use of dipping treatments described here to improve the SWCNT-TCF adhesion on a variety of plastic substrates.

CONCLUSIONS

In the present work, it is demonstrated that the adhesion of SWCNT-TCFs on polymer substrates, specifically PET and PVDF, is improved by dipping the films in nitric acid solutions and NMP, respectively. It has to be emphasized that the immersion methodology is operational with highly resistant thermoplastics such as PVDF. Besides, the R_s values of the SWCNT-TCFs decreased after the immersion treatment, and their transparency increased after a peel-off process. It is also suggested that the SWCNTs would be embedded into both polymer substrates after the treatments. Therefore, the resulting SWCNT layers adhered to the PET and PVDF substrates after the peeling process can be considered as mixed SWCNT/polymer composites. In this way, it would be possible to obtain thin, conductive, and semitransparent SWCNT-TCFs in an easy, cheap, and reproducible way.

DOI: 10.1021/acsomega.8b03475
ACS Omega 2019, 4, 2804−2811

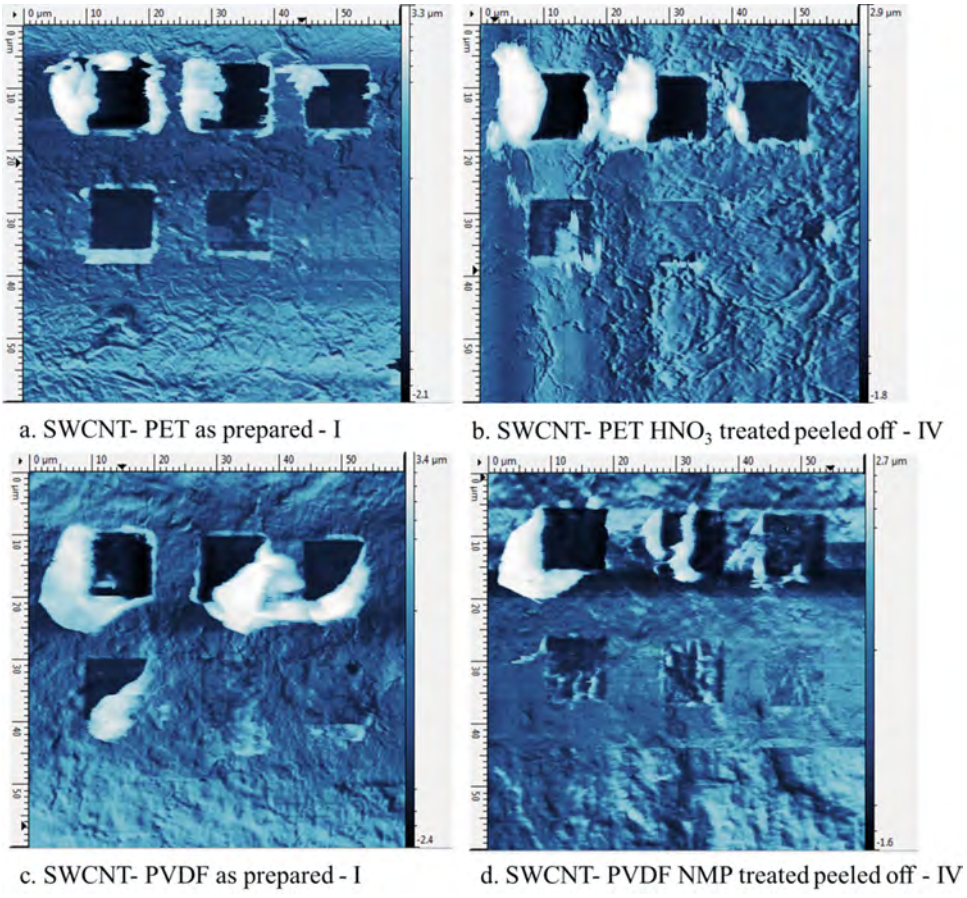

Figure 5. AFM topography images showing the results of scratch tests (forces between 0.5 and 25 μm) on PET (a, b) and PVDF (c, d) before (a, c) and after (b, d) the immersion and peeling-off treatments.

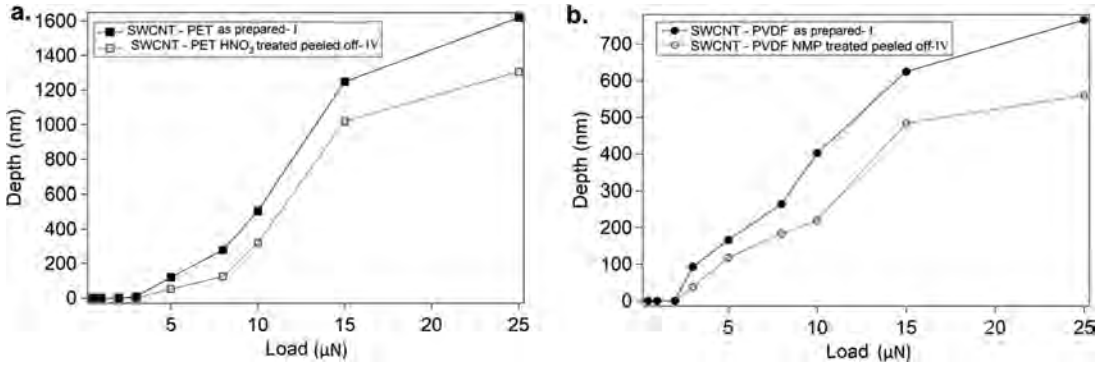

Figure 6. Plots showing variations of depth with the applied load for the SWCNT-PET (a) (squares) and SWCNT-PVDF (b) (circles) films before (full markers) and after (empty markers) the immersion and peeling-off treatments.

Hardness of treated SWCNT coatings improved as compared to the nontreated surfaces. Based on several characterization techniques, it is confirmed that the modification of the SWCNT-TCF during the dipping treatments occurs through analogous mechanisms in both PET and PVDF. Flexible SWCNT-TCF films with improved electrical and adhesion properties can be fabricated in different plastic substrates. Therefore, it can be considered that the immersion procedures described here might be effective on any polymer substrate just by selecting a suitable solvent. The excellent adhesion of the films enables an improved mechanical stability, which is essential for the application of SWCNT-TCFs in electronics.

EXPERIMENTAL SECTION

Materials. Pristine HiPco SWCNTs (diameter 0.8−1.2 nm, length 100−1000 nm, TGA residual mass <35%) were purchased from Nanointegris (Boisbriand, Canada). PET slides, 0.1 mm thick, were supplied by Schwan Stabilo. Flexible PVDF substrates that were 0.1 mm thick were purchased from Goodfellow. Sodium dodecyl sulfate (SDS, ≥98.5%), nitric acid (70%, AR grade), and NMP (99.5%) were provided by Sigma-Aldrich.

Preparation of SWCNT Coatings and Postdeposition Treatments. The starting SWCNT material was dispersed at a concentration of 1 mg mL^{-1} in 0.5% SDS aqueous solutions by 1 h probe sonication (Hielscher UP400S sonicator,

DOI: 10.1021/acsomega.8b03475
ACS Omega 2019, 4, 2804−2811

operating at 60% amplitude and 0.5 cycles). The samples were cooled in an ice-water bath during the sonication process. Next, the SWCNT dispersion was purified by ultracentrifugation at 200 000*g* for 1 h. In this way, the SWCNTs are individualized and purified through the removal of big aggregates, amorphous carbon and metal catalyst impurities, prior to deposition.[36]

Afterward, the purified SWCNT inks were air-sprayed on PET and PVDF substrates using a Sagola Premium 475 spray gun at approximately 1 mL cm^{-2}. The substrates were kept at 50 °C during spray-coating to help water evaporation. To remove the SDS surfactant, the SWCNT-PET and SWCNT-PVDF films were plunged in water for 4 h and dried overnight at room temperature.

The treatment for improving the adhesion was performed by immersion in a plate containing the treatment solution or solvent at room temperature. The SWCNT-PET and SWCNT-PVDF films were dipped in 35−65% HNO_3 and DMF/NMP, respectively, for 5−180 min. Conditions of concentration and time were optimized to produce an adhesion effect while preventing damage of the plastic substrate. Following the immersion, the samples were dried at room temperature overnight.

The adhesion properties of as-sprayed and treated films were in the first place assessed by the simple peel-off tape test using 810 Scotch Magic Tape.

Characterization Techniques. The SWCNT-TCF transparency was assessed by measuring the visible light transmittance (T %) at 550 nm in a Shimadzu UV-2401PC spectrometer. The film thickness was calibrated with a Bruker Stylus Profiler model Dektak XT.

The sheet resistance was measured in a two-probe configuration using a Keithley 4200 unit provided with tungsten needles. Two silver electrodes were painted along the longest sides of each SWCNT-PET and SWNCT-PVDF film. Sheet resistance (R_s) values were calculated taking into account the film geometry, given by the distance between the electrodes and their length.

The homogeneity of the films and the changes caused by the immersion treatment were evaluated by Raman spectroscopy and microscopy techniques. Raman spectra were acquired under ambient conditions using a LabRAM HR Raman spectrometer (Horiba Jobin-Yvon) with a laser excitation energy of 2.33 eV (532 nm). Raman maps of 400 data points were collected with lateral steps of 1 μm, in both X and Y directions, on rectangular areas. Microscopic characterization was conducted in a field emission scanning electron microscope (SEM) model MERLIN (Carl Zeiss, Switzerland), whereas atomic force microscopy (AFM) measurements were carried out in Multimode SPM equipment from Veeco Instruments (Santa Barbara, U.S.).

Scratch Tests. Scratch tests were performed in the Veeco AFM setup with an MPP-13120-10 Bruker AFM probe 8 nm nominal tip radius. The scratch tests were carried out at 2 μm s^{-1} applying various loads (0.5, 1, 2, 3, 5, 8, 10, 15, and 25 μN). Square areas of 10 × 10 μm^2 were scanned at each loading.

The AFM in the topography mode (area 70 × 70 μm^2) was used to examine the surface of the SWCNT-PET and SWCNT-PVDF films before and after the scratch experiments. The topography before the scratch test was used as a reference and subtracted to the final topography. In this way, the starting roughness of the surface is removed and the scratching effect is isolated. To analyze the depths of the scratches, statistical analyses in the whole scratched squares were performed. Histograms of the height inside and outside the scratched squares were taken into account.

AUTHOR INFORMATION

Corresponding Author

*E-mail: alanson@icb.csic.es.

ORCID

Ana M. Benito: 0000-0002-8654-7386

Wolfgang K. Maser: 0000-0003-4253-0758

Alejandro Ansón-Casaos: 0000-0002-3134-8566

Funding

This work has been funded by the MINECO and the European Regional Development Fund (ENE 2016-79282-C5-1-R), the Government of Aragón (T03-17R and E14-17R), and the European Commission (H2020-MSCA-ITN-2014-ETN 642742 "Enabling Excellence").

Notes

The authors declare no competing financial interest.

ACKNOWLEDGMENTS

Special thanks are directed to the Analysis Service at Instituto de Carboquímica ICB-CSIC, particularly to N. Fernández, and SAI at Universidad de Zaragoza.

ABBREVIATIONS

A, absorbance; CNTs, carbon nanotubes; SWCNTs, single-walled carbon nanotubes; PET, poly(ethylene terephthalate); PVDF, poly(vinylidene fluoride); TCFs, transparent conducting films; CVD, chemical vapor deposition; DMF, dimethylformamide; NMP, *N*-methyl-2-pyrrolidone; SEM, scanning electron microscopy; AFM, atomic force microscopy; SDS, sodium dodecyl sulfate; T, transmittance; R_s, sheet resistance; f, adhesion factor; RBM, radial breathing modes; G-band, tangential modes; D-band, disorder mode; d_t, diameter of SWCNTs; R_a, average roughness

REFERENCES

(1) He, H.; Tjong, S. C. Nanostructured transparent conductive films: Fabrication, characterization and applications. *Mater. Sci. Eng., R* **2016**, *109*, 1−101.

(2) Lee, Y.; Ahn, J. Graphene-Based Transparent Conductive Films. *Nano* **2013**, *8*, No. 1330001.

(3) Ansón-Casaos, A.; Mis-Fernández, R.; López-Alled, C. M.; Almendro-López, E.; Hernández-Ferrer, J.; González-Domínguez, J. M.; Martínez, M. T. Transparent conducting films made of different carbon nanotubes, processed carbon nanotubes, and graphene nanoribbons. *Chem. Eng. Sci.* **2015**, *138*, 566−574.

(4) Yu, L.; Shearer, C.; Shapter, J. Recent Development of Carbon Nanotube Transparent Conductive Films. *Chem. Rev.* **2016**, *116*, 13413−13453.

(5) Kaempgen, M.; Duesberg, G. S.; Roth, S. Transparent carbon nanotube coatings. *Appl. Surf. Sci.* **2005**, *252*, 425−429.

(6) Abdelhalim, A.; Abdellah, A.; Scarpa, G.; Lugli, P. Fabrication of carbon nanotube thin films on flexible substrates by spray deposition and transfer printing. *Carbon* **2013**, *61*, 72−79.

(7) Souza, V. H. R.; Flahaut, E.; Zarbin, A. J. G. Conducting, transparent and flexible substrates obtained from interfacial thin films of double-walled carbon nanotubes. *J. Colloid Interface Sci.* **2017**, *502*, 146−152.

(8) Zhang, Q.; Wei, N.; Laiho, P.; Kauppinen, E. I. Recent developments in single-walled carbon nanotubes thin films fabricated by dry floating catalyst chemical vapor deposition. *Top. Curr. Chem.* **2017**, *375*, 90.

DOI: 10.1021/acsomega.8b03475
ACS Omega 2019, 4, 2804−2811

(9) Park, S.; Vosguerichian, M.; Bao, Z. A review of fabrication and applications of carbon nanotube film-based flexible electronics. *Nanoscale* **2013**, *5*, 1727−1752.
(10) Majumder, M.; Rendall, C.; Li, M.; Behabtu, N.; Eukel, J. A.; Hauge, R. H.; Schmidt, H. K.; Pasquali, M. Insights into the physics of spray coating of SWNT films. *Chem. Eng. Sci.* **2010**, *65*, 2000−2008.
(11) Jung, H.; An, S. Y.; Lim, J. S.; Kim, D. Transparent Conductive Thin Film Synthesis Based on Single-Walled Carbon Nanotubes Dispersion Containing Polymethylmethacrylate Binder. *J. Nanosci. Nanotechnol.* **2011**, *11*, 6345−6349.
(12) Lim, S. C.; Choi, H. K.; Jeong, H. J.; Song, Y. L.; Kim, G. Y.; Jung, K. T.; Lee, Y. H. A. Strategy for Forming Robust Adhesion With the Substrate in a Carbon-Nanotube Field-Emission Array. *Carbon* **2006**, *44*, 2809−2815.
(13) Pei, S.; Du, J.; Zeng, Y.; Liu, C.; Cheng, H. M. The Fabrication of a Carbon Nanotube Transparent Conductive Film by Electrophoretic Deposition and Hot-Pressing Transfer. *Nanotechnology* **2009**, *20*, 235707−235713.
(14) Shim, H. C.; Kawk, Y. K.; Han, C. S.; Kim, S. Enhancement of Adhesion Between Carbon Nanotubes and Polymer Subtrates Using Microwave Irradiation. *Scr. Mater.* **2009**, *61*, 32−35.
(15) Azoubel, S.; Magdassi, S. Controlling Adhesion Properties of SWCNT-PET Films Prepared by Wet Deposition. *ACS Appl. Mater. Interfaces* **2014**, *6*, 9265−9271.
(16) Parekh, B. B.; Fanchini, G.; Eda, G.; Chhowalla, M. Improved conductivity of transparent single-wall carbon nanotube thin films via stable postdeposition functionalization. *Appl. Phys. Lett.* **2007**, *90*, No. 121913.
(17) Geng, H. Z.; Lee, D. S.; Kim, K. K.; Han, G. H.; Park, H. K.; Lee, Y. H. Absorption spectroscopy of surfactant-dispersed carbon nanotube film: modulation of electronic structures. *Chem. Phys. Lett.* **2008**, *455*, 275−278.
(18) Paul, S.; Kim, D. W. Preparation and characterization of highly conductive transparent films with single-walled carbon nanotubes for flexible display applications. *Carbon* **2009**, *47*, 2436−2441.
(19) Jeong, H.; Park, J. Y. Local electrical investigations of nitric acid treatment effects on carbon nanotube networks. *J. Phys. Chem. C* **2015**, *119*, 9665−9668.
(20) Stern, A.; Azoubel, S.; Sachyani, E.; Livshits, G. I.; Rotem, D.; Magdassi, S.; Porath, D. Conductivity Enhancement of Transparent 2D Carbon Nanotube Networks Occurs by Resistance Reduction in All Junctions. *J. Phys. Chem. C* **2018**, *122*, 14872−14876.
(21) Begum, S.; Kausar, A.; Ullah, H.; Siddiq, M. Potential of polyvinylidene fluoride/carbon nanotube composite in energy, electronics, and membrane technology: an overview. *Polym.-Plast. Technol. Eng.* **2016**, *55*, 1949−1970.
(22) Chen, X.; Han, X.; Chen, Q. D. PVDF-based ferroelectric polymers in modern flexible electronics. *Adv. Electron. Mater.* **2017**, *3*, No. 1600460.
(23) Puértolas, J. A.; García-García, J. F.; Pascual, F. J.; González-Domínguez, J. M.; Martínez, M. T.; Ansón-Casaos, A. Dielectric behavior and electrical conductivity of PVDF filled with functionalized single-walled carbon nanotubes. *Compos. Sci. Technol.* **2017**, *152*, 263−274.
(24) Bottino, A.; Capannelli, G.; Munari, S.; Turturro, A. Solubility parameters of poly(vinylidene fluoride). *J. Polym. Sci., Part B: Polym. Phys.* **1988**, *26*, 785−794.
(25) Lee, S. W.; Kim, K. K.; Cui, Y.; Lim, S. C.; Cho, Y. W.; Kim, S. M.; Lee, Y. H. AdhesionTest Of Carbon Nanotube Film Coated Onto Transparent Conducting Substrates. *Nano* **2010**, *5*, 133−138.
(26) Itkis, M. E.; Pekker, A.; Tian, X.; Bekyarova, E.; Haddon, R. C. Networks of semiconducting SWNTs: contribution of midgap electronic states to the electrical transport. *Acc. Chem. Res.* **2015**, *48*, 2270−2279.
(27) Li, H.; Geng, H. Z.; Meng, Y.; Wang, Y.; Xu, X. B.; Ding, E. X.; Gao, J.; Chen, L. T.; Ma, S. Fabrication and test of adhesion enhanced flexible carbon nanotube transparent conducting films. *Appl. Surf. Sci.* **2014**, *313*, 220−226.
(28) Tsai, W.-L.; Wang, K. Y.; Chang, Y. J.; Li, Y. R.; Yang, P.-Y.; Chen, K. N.; Cheng, H. C. Conductivity enhancement of multiwalled carbon nanotube thin film vis thermal compression method. *Nanoscale Res. Lett.* **2014**, *9*, 451.
(29) Shimizu, M.; Fuji, S.; Tanaka, T.; Kataura, H. Effects of surfactants on the electronic transport properties of thin-film transistors of single-wall carbon nanotubes. *J. Phys. Chem. C* **2013**, *117*, 11744−11749.
(30) Seeger, T.; Fuente, G.; Maser, W. K.; Benito, A. M.; Callejas, M. A.; Martínez, M. T. Evolution of multiwalled carbon-nanotube/SiO_2 composites via laser teatment. *Nanotechnology* **2003**, *14*, 184−187.
(31) Araujo, P. T.; Pesce, P. B. C.; Dresselhaus, M. S.; Sato, K.; Saito, R.; Jorio, A. Resonance Raman spectroscopy of the radial breathing modes in carbon nanotubes. *Phys. E* **2010**, *42*, 1251−1261.
(32) Kataura, H.; Kumazawa, Y.; Maniwa, Y.; Umczu, I.; Suzuki, S.; Ohtsuka, Y.; Achiba, Y. Optical properties of single-wall carbon nanotubes. *Synth. Met.* **1999**, *103*, 2555−2558.
(33) Bergeret, C.; Cousseau, J.; Fernandez, V.; Mevellec, J.; Lefrant, S. Spectroscopic Evidence of Carbon Nanotubes' Metallic Character Loss Induced by Covalent Functionalization via Nitric Acid Purification. *J. Phys. Chem. C.* **2008**, *112*, 16411−16416.
(34) Pimenta, M. A.; Marucci, A.; Empedocles, S. A.; Bawendi, M. G.; Hanlon, E. B.; Rao, A. M.; Eklund, P. C.; Smalley, R. E.; Dresselhaus, G.; Dresselhaus, M. S. Raman modes of metallic Carbon nanotubes. *Phys. Rev. B* **1998**, *58*, No. R16016.
(35) Voggu, R.; Rout, C. S.; Franklin, A. D.; Fisher, T. S.; Rao, C. N. R. Extraordinary Sensitivity of The Electronic Structure and Properties of Single-Walled Carbon Nanotubes to Molecular Charge-Transfer. *J. Phys. Chem. C* **2008**, *112*, 13053−13056.
(36) Ansón-Casaos, A.; González-Domínguez, J. M.; Lafragüeta, I.; Carrodeguas, J. A.; Martínez, M. T. Optical absorption response of chemically modified single-walled carbon nanotubes upon ultracentrifugation in various dispersants. *Carbon* **2014**, *66*, 105−118.

DOI: 10.1021/acsomega.8b03475
ACS Omega 2019, 4, 2804−2811